Raman study of one-dimensional spin fluctuations in the spin-1 Heisenberg-chain compound Y_2BaNiO_5: Contrast with simple expectations

P. E. Sulewski and S-W. Cheong

AT&T Bell Laboratories, 600 Mountain Avenue, Murray Hill, New Jersey 07974-0636

(Received 21 March 1994; revised manuscript received 6 October 1994)

Spin fluctuations in the Haldane ground state should exhibit a quantum spin gap observable with Raman scattering. The Raman spectra of single-crystalline Y_2BaNiO_5, a linear spin-1 Heisenberg antiferromagnet, exhibit broad continuum scattering between ~ 200 and ~ 800 cm^{-1}, in the energy range expected for magnetic excitations ($\sim J = 224$ cm^{-1}). Numerous weak and broad features superimposed on this continuum scattering possibly result from quantization of the magnon continuum by local molecular fields from nearby chains. A strong and relatively narrow mode at ~ 680 cm^{-1}, near $3J$, unrelated to lattice vibrations, may also be of magnetic origin. All of these features are strongly resonant in the red ($\lambda_L = 6328$ Å), disappearing for shorter excitation wavelengths. These spectra provide a view of the Haldane spin system excitations complementary to that given by inelastic neutron scattering. Modeling the excitations with Schwinger bosons or spin waves predicts a highly asymmetric scattering feature with a sharp onset near $2\Delta(\sim 0.8J)$, gradually diminishing toward higher energies. The observed spectra disagree with this theoretical expectation, perhaps due to spin-phonon coupling which may provide an efficient decay channel for the magnon pairs.

I. INTRODUCTION

The interactions underlying the Haldane spin system can be quite succinctly stated in the familiar Heisenberg model:

$$H = J \sum_{\langle ij \rangle} \mathbf{S}_i \cdot \mathbf{S}_j \, . \tag{1}$$

This deceptively simple Hamiltonian has been extensively studied experimentally and theoretically.[1] In the case of the spin-1 linear Heisenberg chain, Haldane's prediction of a finite gap above a singlet ground state[2] has been verified through numerical simulations[3] and experimental realizations.[4]

Inelastic neutron-scattering experiments on $Ni(C_2H_8N_2)_2NO_2CiO_4$ (NENP) (Ref. 5) demonstrate the existence of a gap and of magnonlike excitations which can be well-represented by the single-mode approximation (SMA). This inelastic light-scattering experiment probes transitions between the ground and excited states in the subspace of eigenfunctions orthogonal to those probed in the one-magnon neutron scattering. Thus the spectra presented in this paper provide a view of the manifold of excited states complementary and orthogonal to that presented by the inelastic neutron-scattering data. In principle, the quantum spin gap and the multimagnon continuum, which has not been observed, should appear in the Raman spectra.

If the excited-state manifold were well-represented by SMA, our spectra would be described in terms of two-magnon Raman scattering. In this case the Raman spectra would be derived from the dispersion curve identified by inelastic neutron scattering. This procedure does not reproduce the features observed in the Raman scattering of the Haldane system. The Raman spectra presented here therefore provide a challenge to schemes which pur-

port to represent the excitations of the Haldane system.

This situation is similar to the case of the planar cuprates, where, again, inelastic neutron scattering finds well-defined spin waves,[6] while the spin-pair scattering exhibits significant deviations from spin-wave theory predictions.[7]

II. EXPERIMENTAL DETAILS

The structure of Y_2BaNiO_5, dominated by isolated chains of compressed NiO_6 octahedra, suggests that the magnetic properties may be well-described by the theoretical one-dimensional (1D) $S = 1$ Heisenberg antiferromagnet (AFM). The shortened Ni-O bond length along the chains leads to a large superexchange interaction, $J \sim 322$ K (224 cm^{-1}), between nearest-neighbor Ni spins along the chains.[8] Recent magnetic-susceptibility data[9] clearly identify Y_2BaNiO_5 as a new Haldane state compound with a spin gap of ~ 100 K. Deviations from isotropy lead to a splitting of the excited triplet state, and the system can be described by a 1D Hamiltonian with planar anisotropy:

$$H = J \sum_i \mathbf{S}_i \cdot \mathbf{S}_{i+1} + D \sum_i (S_i^z)^2 \tag{2}$$

with $D \sim 0.2J$. Alternatively, the splitting may arise from exchange anisotropy ($J_z \neq J_{x,y}$). In either case, anisotropy prevents the scattering Hamiltonian, H_R, from commuting with H, ensuring inelastic scattering.

Single crystals of Y_2BaNiO_5 and Gd_2BaNiO_5 grown out of a BaO-NiO rich flux, have dimensions up to $5 \times 2 \times 0.3$ mm, with the longest dimension along the spin chains. Residual flux on the crystal surfaces is removed with bromine/methanol etch, resulting in highly reflective faces.

Several lasers are employed to span the region of the optical gap for resonance conditions. Resonant enhancement of the apparent spin-fluctuation scattering is achieved in the red, excited with ~10 mW of 6328 Å light from a HeNe laser. A Dilor XY spectrometer with a liquid-nitrogen-cooled Thomsen 1024×256 charge-coupled-device camera records the Raman spectra in backscattering. Samples mounted with silver paste on a silicon substrate are cooled between 12 K and room temperature in a Janis SVT cryostat.

III. DATA

The spectra in Fig. 1 show the resonance behaviors of the Raman modes with excitation energies between 2.0 and 2.8 eV, for the sample temperature at ~20 K. The incident and scattered electric fields are along the Ni-O chains (a axis). Extraneous peaks due to residual plasma fluorescence from the laser are marked with asterisks. The top spectrum is obtained with ~5 mW of 4416 Å from a HeCd laser, the next five spectra with ~40 mW at 4545, 4579, 4658, 4880, and 5145 Å from an Ar⁺ ion laser, and the bottom spectrum with ~10 mW at 6328 Å from a HeNe. Reducing the laser power to below 3 mW does not change the spectra.

Although the intensities of the spectra are shown with arbitrary units, and hence cannot be compared, certain features are clearly resonant. For example, the overall broad background which peaks at ~500 cm⁻¹ appears to be strongest at 6328 Å. Actually, as the laser excitation frequency increases, the spectral resolution decreases from 5 to 13 cm⁻¹, since the slit width remains 150 μm. This change in resolution can be seen by noting the width of the plasma lines. Since a reduction in resolution enhances broad features, the broad resonance at 6328 Å is even stronger than appears in Fig. 1.

The most intense peak in the 6328 Å spectrum at 681 cm⁻¹ and its weaker satellite at ~705 cm⁻¹ shrink quite dramatically with increasing excitation frequency, disappearing nearly completely in the 4658 Å spectrum. The mode at 774 cm⁻¹ and its satellite at 758 cm⁻¹ exhibit the opposite resonance behavior, appearing strong through the blue and weakening significantly at 5145 Å, nearly disappearing at 6328 Å. We have previously identified the sharp modes at 235 and 541 cm⁻¹ as A_g phonons, and the weaker mode at 432 cm⁻¹ as a "leak" of a very intense B_{3g} phonon.[10]

Comparing the spectra of Y_2BaNiO_5 with those of the isostructural Gd_2BaNiO_5, shown in Fig. 2, provides further help in identifying the various Raman features. In Gd_2BaNiO_5, the Gd magnetic moment interferes with the
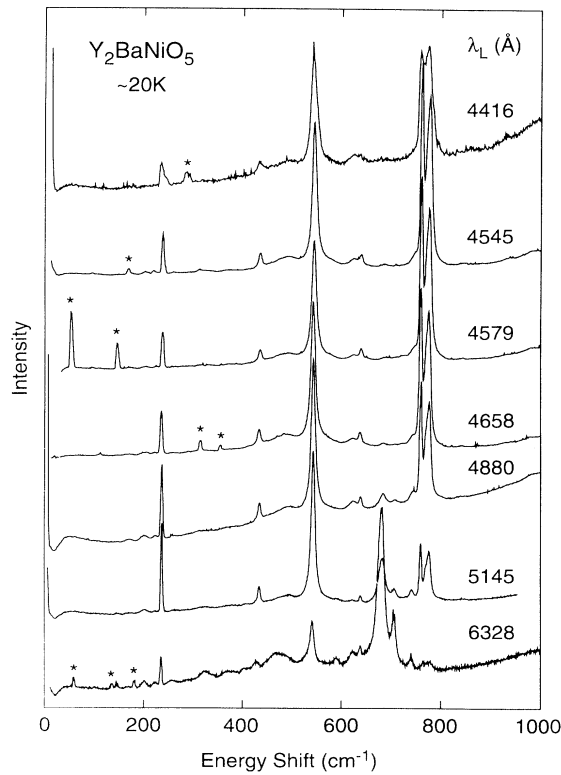

FIG. 1. Raman spectra of Y_2BaNiO_5 at ~20 K for several incident laser wavelengths with incident and scattered electric fields along the Ni-O(2) chains. Asterisks mark irrelevant laser plasma lines.
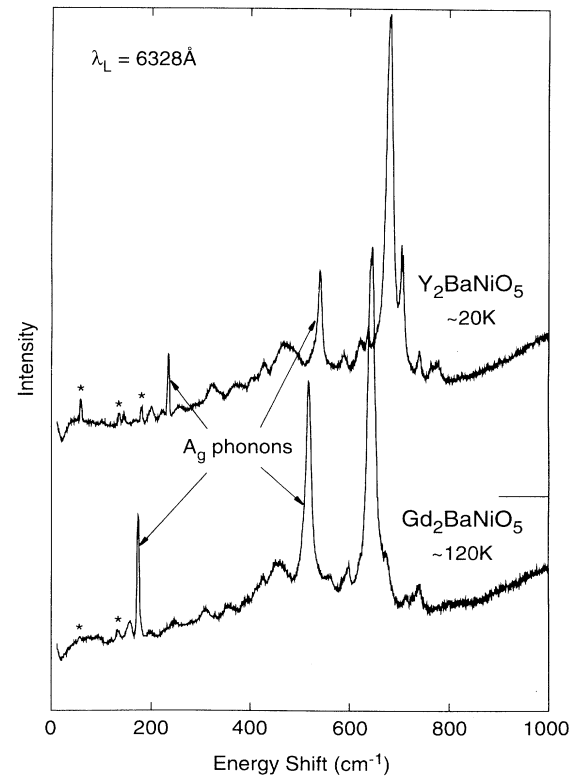
FIG. 2. Comparison or Raman spectra of Y_2BaNiO_5 at ~20 K and Gd_2BaNiO_5 at ~120 K with $\lambda_L = 6328$ Å. The Gd_2BaNiO_5 spectrum remains essentially the same at lower temperature. Plasma lines from the laser are marked with asterisks.

development of the Haldane ground state. Instead, Gd_2BaNiO_5 exhibits a three dimensionally magnetically ordered ground state. Thus any structure appearing in the Y_2BaNiO_5 spectra reflecting the Haldane gap should be absent in the Gd_2BaNiO_5 spectra. Figure 2 shows that nearly all of the features are common to the spectra of Gd_2BaNiO_5 and Y_2BaNiO_5, albeit at slightly different frequencies. Table I lists the frequencies of the most prominent modes for low temperature ($R = Y$ at $\sim 20K, R = Gd$ at ~ 120 K) and also at room temperature (not shown in figures). The sharp A_g phonons at 174 and 235 cm^{-1} due to vibrations of the Gd and Y, respectively, shift as the square root of the ionic mass. The O(1) related A_g phonon at 541 cm^{-1} in Y_2BaNiO_5 shifts to 518 cm^{-1} in Gd_2BaNiO_5, consistent with the slightly larger bond distances in the latter compound. Between these A_g phonons, the broad irregular structure appears quite similar for the two spectra of Fig. 2. These numerous small features appear superimposed on a broad continuum between ~ 200 and ~ 800 cm^{-1}. A similar multitude of features in the Raman spectra of the 1D Ising-like antiferromagnets $CsCoCl_3$ and $CsCoBr_3$ (Ref. 11) is attributed to quantization of the magnon continuum by local molecular fields from nearby chains.[12] Although this interpretation relies on the Ising-like interactions in $CsCoCl_3$ and $CsCoBr_3$, similar narrow structures are also observed in the 1D AFM $CsNiCl_3$,[13] which exhibits a more isotropic exchange.

The most intense features in Fig. 2 occur at 681 cm^{-1} with a well-resolved satellite at 705 cm^{-1} for Y_2BaNiO_5, and at 645 cm^{-1} with a shoulder at ~ 674 cm^{-1} for Gd_2BaNiO_5. As mentioned above, these features are strongly resonantly enhanced in the red. With higher laser excitation energy these features disappear, while a strong mode at 774 (741) cm^{-1} with a satellite at 758 (728) cm^{-1} develops for Y_2BaNiO_5 (Gd_2BaNiO_5). At room temperature all of the modes broaden and soften slightly ($\sim 1\%$), by similar amounts for two materials. The only exception is the 681-cm^{-1} mode in Y_2BaNiO_5, which softens by ~ 16 cm^{-1}, while the corresponding mode in Gd_2BaNiO_5 softens by only ~ 10 cm^{-1}. Some of

these features may be Raman-forbidden infrared (IR)-active modes made allowed by defects. For example, a strong IR-active band occurs in *Immm* Tm_2BaNiO_5 at 786 cm^{-1}.[14] Defects along the Ni-O(2) chain break the inversion symmetry at the Ni and O(2) sites, inducing Raman activity of this mode. For the single crystals, which are flux grown at high temperatures in Pt crucibles, some number of Ni ions are replaced by Pt. The polycrystalline samples, grown by solid-state diffusion at lower temperatures, have no Pt on the Ni sites. In Raman spectra of polycrystalline samples of Y_2BaNiO_5 and other isostructural materials these intense modes above 600 cm^{-1} only appear weakly, if at all.[15]

Figure 3 shows the Raman spectra for Y_2BaNiO_5 at ~ 20 K. Again, the asterisks mark the position of plasma lines from the HeNe laser. The spectra are labeled *xx*, for the incident and scattered electric fields along the chain axis, *yy*, for the electric fields parallel to each other and perpendicular to the chain axis, and *xy*, for one electric field along the chain axis and one perpendicular to this axis. The underlying broad structure exhibited by the *xx*, and to some extent by the *yy*, spectrum is reminiscent of the broad spin-fluctuation spectrum observed for La_2CuO_4 and the other insulating planar cuprates. This broad continuum scattering exhibits a cutoff at
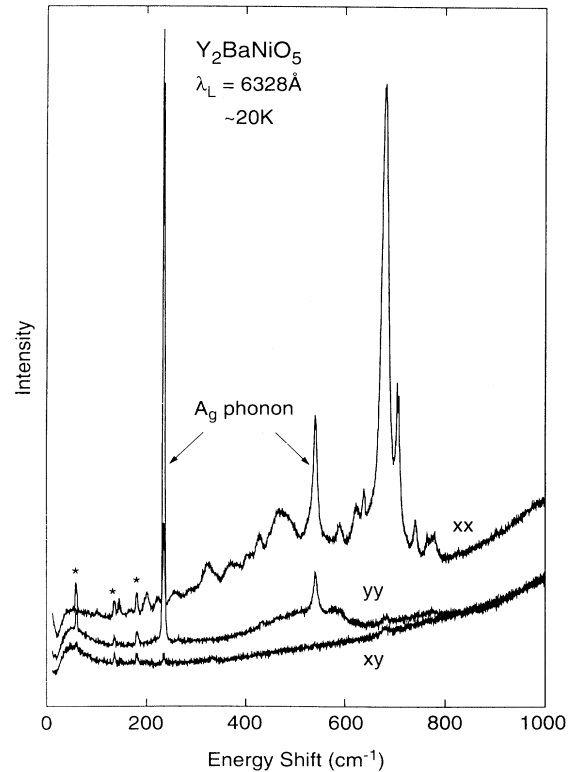
TABLE I. Frequencies (in cm^{-1}) of some prominent modes appearing in the spectra of Y_2BaNiO_5 at ~ 20 K and room temperature and Gd_2BaNiO_5 at ~ 120 K and room temperature. Features for the Gd_2BaNiO_5 remains essentially constant for temperatures below 120 K.

Origin	Y (20 K)	Y (300 K)	Gd (120 K)	Gd (300 K)
A_g phonon	235	232	174	172
B_{3g} phonon	432	431	424	422
A_g phonon	541	539	518	517
	622			
	637			
Magnetic?	681	665	645	635
	705		674	
	740			
IR?	758	748	728	719
IR?	774	761	741	730

FIG. 3. Raman spectra of Y_2BaNiO_5 at ~ 20 K for three polarization combinations: incident and scattered electric fields along the chain axis (*xx*), perpendicular to the chain axis (*yy*), and crossed with one field along the chain and one perpendicular (*xy*).

~ 800 cm^{-1} in both xx and yy spectra. From the band-width of the dispersion,[5] we expect this cutoff to be $\sim 5.4J \approx 1200$ cm^{-1} for two-magnon scattering. Defect-allowed single-magnon scattering should show a cutoff at $\sim 2.7J \approx 600$ cm^{-1}, and may provide a plausible explanation for this continuum. Interestingly, the ratio of the anti-Stokes to Stokes spectra at room temperature for 6328 Å excitation closely follows the expected $e^{-\hbar\omega/kT}$ up to $|\omega| \sim 700$ cm^{-1}, indicating that even the background intensity is true Raman scattering. This result suggests that all of the intensity in the low-temperature spectra of Fig. 3 is Raman scattering and not fluorescence. While real, however, some scattering may be defect-induced and not relevant to the spin-fluctuation scattering.

IV. DISCUSSION

In general, light can couple to spins through the spin-orbit interaction, leading to one-magnon scattering, or through an excited-state exchange interaction, resulting in spin pair (two-magnon) scattering.[16] The effective interaction Hamiltonian for the latter process takes the form[17]

$$H_R = \sum_{\langle ij \rangle} (\mathbf{E}_1 \cdot \overset{\leftrightarrow}{\mathbf{C}} \cdot \mathbf{E}_2)(\mathbf{S}_i \cdot \mathbf{S}_j) , \qquad (3)$$

where $\overset{\leftrightarrow}{\mathbf{C}}$ is a tensor determined by symmetry considerations. We note that this effective Hamiltonian describing the Raman scattering does have potentially large uncertainties (e.g., the magnitude of the coupling, large second neighbor terms, etc.). Since the spin function transforms like A_g, the tensor $\overset{\leftrightarrow}{\mathbf{C}}$ must be diagonal, coupling the electric-field components by $E_1^\alpha E_2^\alpha$, where $\alpha = x, y, z$. Thus, spin-pair scattering should only be observed for polarized scattering ($\mathbf{E}_1 \| \mathbf{E}_2$).

For the isotropic system ($D = 0$), the magnetic Hamiltonian [Eq. (2)] commutes with the nearest neighbor (NN) interaction Hamiltonian ($j = i + 1$). Thus no scattering results from the NN spin-flip term for an isotropic system. Next-nearest-neighbor (NNN) scattering, corresponding to $\sum \mathbf{S}_i \cdot \mathbf{S}_{i+2}$, is allowed, although no doubt with a greatly reduced matrix element. For the case at hand, however, the significant planar anisotropy allows the NN scattering process.

Spin-wave theory (SWT) attempts to represent the important lowest-lying excitations by generating states from the ground state, $|0\rangle$, through applications of the spin-wave creation operators $\alpha_{\uparrow k}^\dagger$ and $\alpha_{\downarrow k}^\dagger$. In terms of these operators, the interaction Hamiltonian, H_R [Eq. (3)], may be written

$$H_R = \sum_k \cos(k)(u_k^2 + v_k^2)\alpha_{\uparrow k}^\dagger \alpha_{\downarrow -k}^\dagger . \qquad (4)$$

From this expression, H_R corresponds to the creation of a pair of magnons with zero total spin and momentum. The resulting Raman spectrum for $T = 0$ K is given by

$$I(\omega) = \sum_k |\langle k | H_R | 0 \rangle|^2 \delta(\omega - 2\varepsilon_k) . \qquad (5)$$

If the matrix element does not vary over k, the spectrum reflects the density of states for creation of a zero momentum pair of magnons. We obtain a crude approximation for $I(\omega)$ by replacing the SWT ε_k with the dispersion curve experimentally obtained for NENP:[5]

$$\varepsilon_k^2 = \Delta^2 + c^2 \sin^2 k + A \cos^2(k/2) , \qquad (6)$$

with $\Delta = 0.4J, c = 2.5J$, and $A = 2J^2$. The resulting spectrum is shown as the solid curve in Fig. 4(a). The divergent peaks at $\sim 0.8J$ (180 cm^{-1}) and $\sim 3.0J$ (672 cm^{-1}) result from the flatness of the dispersion curve near the zone boundary and zone center, respectively. No peak occurs from the dispersion curve maximum at $k = \pi/2$ because of the $\cos^2 k$ geometric factor in the matrix element. Since the portion of the dispersion curve for $|q| < 0.3\pi$ lies within the two-magnon continuum, well-defined magnons are neither expected[18] nor observed[5] near the zone center. Thus, only the peak at $\sim 0.8J$ (180 cm^{-1}) should be present. The anisotropy will split this peak into two peaks separated by $\sim 3D$,[19] since H_R [Eq. (3)] preserves S_{total}^z.

Magnon interactions typically broaden and shift peaks calculated assuming noninteracting magnons.[20] For many magnetic systems interaction effects can shift the peak in the spectrum down by $\sim J$. The importance of magnon interactions is gauged by the parameter $\theta = 1/Sz$, where z is the coordination number. For the $S = 1$ spin chain, $\theta = \frac{1}{2}$, which is the same as the value for the spin-$\frac{1}{2}$ planar cuprates, where interactions strongly modify the scattering spectrum.[7] In the classical limit ($S \to \infty$), interactions can be ignored. Attempts have been made, with apparent success, to calculate interaction effects with approximate Green-function methods.[20] Applying this approximation to the spin-1 chain yields
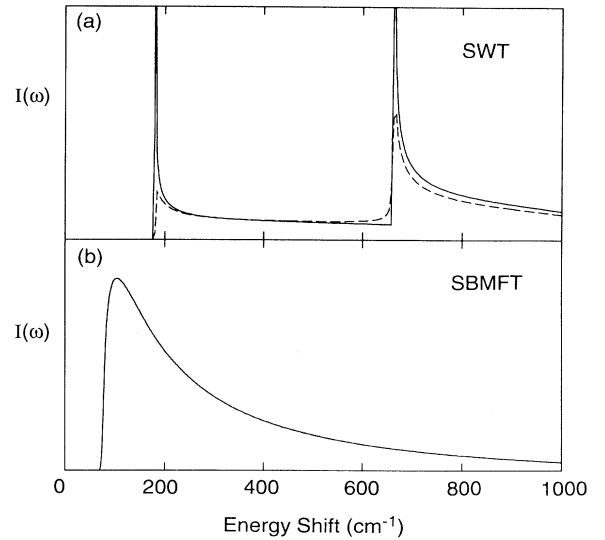

FIG. 4. Theoretical expectation for Raman spectrum of Haldane system, predicted from (a) spin-wave theory (SWT) (solid) and SWT with interactions (dashed) and (b) Schwinger-boson mean-field theory.

the dashed curve in Fig. 4(a). Interactions naturally reduce the divergences and broaden the spectrum slightly, however, no major shifts in peak position are produced. Numerical studies of the $q = \pi$ magnons find the magnon-magnon interactions are small and repulsive in the relevant singlet channel, shifting the peak at $\sim 0.8J$ toward slightly higher energy.[18]

Another approximation to the spin fluctuation spectrum can be obtained from the Schwinger-boson mean-field theory (SBMFT) of Arovas and Auerbach.[21] The spin operators in H_R are replaced by the Schwinger boson operators so that

$$H_R = a_i^\dagger b_i a_j b_j^\dagger + a_i b_i^\dagger a_j^\dagger b_j \; . \tag{7}$$

Employing the spinon operators,[22] which by a Bogoliubov–de Gennes transformation diagonalize the mean-field Hamiltonian, we calculate the spectrum which appears in Fig. 4(b). The onset of scattering occurs at ≈ 74 cm^{-1}, reflecting the failure of SBMFT to accurately predict the magnitude of the Haldane gap.

A more legitimate calculation of the spin-fluctuation scattering can be made using the field-theoretical description of Affleck and Weston,[23] which agrees very well with recent numerical calculations by Sorensen and Affleck,[24] although such a calculation is beyond the scope of this paper. However, following Affleck and Weston,[23] we can treat the elementary excitations of the spin chain in the so-called free-boson approximation, where the energy-momentum relation is

$$\varepsilon_k = \sqrt{\Delta^2 + v^2(k - \pi)^2} \; . \tag{8}$$

As in the spin-wave case, the spectrum arises from boson pair creation, and, assuming that the matrix element depends only weakly on momentum, the intensity should be roughly proportional to the two-boson density of states:

$$I(\omega) \propto \rho(\omega) = \sum_k \delta(\omega - 2\varepsilon_k)$$

$$\propto \begin{cases} \dfrac{\omega}{\sqrt{\omega^2 - (2\Delta)^2}} & \text{for } \omega \geq 2\Delta \\ 0, \text{ otherwise} \; . \end{cases} \tag{9}$$

Thus the spectrum has a threshold at 2Δ with a square-root singularity, similar to the previous approximations shown in Fig. 4.

Comparing Fig. 4 with the data in Fig. 3 shows that none of the approximation schemes reproduces the observed spectra. Although anisotropy will split the mode at 2Δ, the absence of spectral weight or structure in the spectra near 2Δ cannot be explained. Rather than peaking near 2Δ (~ 180 cm^{-1}), the spectra are relatively flat through this region, and instead broadly peak near ~ 500 cm^{-1}. An exact diagonalization of a 12-site chain with $D = 0.2J$ gives a set of discrete states for the spectrum [Eq. (5)], consistent with the above two models.[25] However, even with $D = 0.2J$, most of the spectral weight is at zero frequency, and hence the intensity of the spin-fluctuation scattering is expected to be small.[25] This fact

may explain the absence of the expected feature, but does not clarify the structure that is observed. In addition, SWT and SBMFT do not represent the midzone excitations very well.[26] Since the spectral weight at higher energy comes from midzone excitations, the model calculations are probably unreliable much above the spin gap.

An alternative explanation for the disparity between the simple theoretical expectation and the observed spectrum is spin-phonon coupling.[27] Lattice vibrations couple to the spin degrees of freedom by modulating the exchange energy, J, which depends strongly on the interatomic distances. The effects of such coupling on the spin-pair scattering have been recently demonstrated[28] for the antiferromagnet FeBO$_3$. This coupling could provide a mechanism for broadening the spin-fluctuation spectrum, as well as a description of the continuum scattering observed. An analogous situation exists in the Raman spectra of the planar cuprate superconductors in the region of the superconducting energy gap. In this case a clear threshold for scattering is expected, but not observed,[29] and the coupling of quasiparticles to phonons has been invoked as an explanation.[30]

Although not predicted by the above models, simple arguments suggest that a two-magnon Raman mode should generally occur near $(2Sz - 1)J$.[31] This estimate works quite well for a variety of antiferromagnets, including three-dimensional systems [e.g., RbMnF$_3$ ($S = \frac{5}{2}$) (Ref. 32) and KNiF$_3$ ($S = 1$) (Ref. 33)] and two-dimensional systems [e.g., K$_2$NiF$_4$ ($S = 1$) (Ref. 34) and La$_2$CuO$_4$ ($S = \frac{1}{2}$) (Ref. 7)]. In these cases, this two-magnon mode near $(2Sz - 1)J$ arises from the large density of states of magnon pairs at the zone boundary, where $2\varepsilon_k = 2SzJ$ [cf. Eq. (5)], shifted down by $\sim J$ by the previously mentioned magnon-magnon interactions. For the spin chain, the contribution to the scattering from the dispersion curve maximum is suppressed, as discussed above, yet the simple local arguments leading to the peak at $(2Sz - 1)J$ are not obviously invalidated.

For the $S = 1$ spin chain, with coordination number, $z = 2$, this mode is at $3J$. For a heuristic picture, consider a 1D spin-1 Ising system in the Néel ground state:

$$\cdots \downarrow - \uparrow - \downarrow - \uparrow - \downarrow - \uparrow \cdots \; .$$

The energy of this state is $-Jn$. Now consider the Raman process which changes the spins of a nearest-neighbor pair by ± 1:

$$\cdots \downarrow - \uparrow - \bullet - \bullet - \downarrow - \uparrow \cdots \; .$$

The energy of this state is $-J(N - 3)$, and the energy difference is $3J$. For Y$_2$BaNiO$_5$, $3J = 672$ cm^{-1}, remarkably close to the chain-polarized mode observed at 681 cm^{-1}. The corresponding mode for Gd$_2$BaNiO$_5$ occurs at 645 cm^{-1}. Unlike the mode at 774 (741) cm^{-1} in Y$_2$BaNiO$_5$ (Gd$_2$BaNiO$_5$), there is no IR-active mode observed between ~ 600 and ~ 750 cm^{-1},[14] making it unlikely that this feature is simply an IR-active mode appearing in Raman due to disorder. Since the Ni-O(2) bond distance for $R =$ Gd is 0.70% larger than for $R =$ Y, the superexchange along this bond should be smaller for $R =$ Gd, leading to a reduced value of J, consistent with

the behavior of this Raman mode. More quantitatively, among isostructural systems, the exchange parameter, J, often exhibits a power-law dependence on bond length, $J \propto d^{-n}$. For the relatively weak superexchange antiferromagnets X_2MF_4 ($X = K, Rb, Tl; M = Mn, Co, Ni$), $n \sim 12$.[35] For the planar cuprates, which have very strong superexchange, $n \sim 4$.[36] Attributing the Raman mode at 681 (645) cm^{-1} in Y_2BaNiO_5 (Gd_2BaNiO_5) to a magnetic excitation results in $n \sim 8$, a reasonable value. The rather small width ($\sim 3\%$ full width at half maximum) of these Raman modes would seem opposed to their interpretation as two-magnon excitations, however.

V. CONCLUSIONS

Inelastic neutron-scattering results[5] suggest that the $\Delta S = 1$ excitations of the Haldane spin system obey the single-mode approximation (SMA). $\Delta S = 0$ spin-pair modes calculated from the SMA predict a feature at $2\Delta (\sim 0.8J)$, which does not correlate with features observed in the Raman spectra of Y_2BaNiO_5. The numerous weak and broad structures experimentally observed are not expected within the SMA, but may reflect quantization of the expected spin-fluctuation continuum by local molecular fields.[12]

ACKNOWLEDGMENTS

[1]L. J. de Jongh and A. R. Miedema, Adv. Phys. **23**, 1 (1974); M. Steiner, J. Villain, and C. G. Windsor, Adv. Phys. **25**, 87 (1976); J. P. Renard, S. Clement, and M. Verdaguer, Proc. Indian Acad. Sci. (Chem. Sci.) **98**, 131 (1987).

[2]F. D. M. Haldane, Phys. Lett. **93A**, 464 (1983); Phys. Rev. Lett. **50**, 1153 (1983).

[3]M. Takahashi, Phys. Rev. Lett. **62**, 2313 (1989); M. P. Nightingale and H. W. J. Blote, Phys. Rev. B **33**, 659 (1986); S. R. White and D. A. Huse, Phys. Rev. B **48**, 3844 (1993).

[4]W. J. L. Buyers *et al.*, Phys. Rev. Lett. **56**, 371 (1986); Z. Tun *et al.*, Phys. Rev. B **42**, 4677 (1990); L. P. Regnault *et al.*, Physica B **156-157**, 247 (1989); K. Katsumata *et al.*, Phys. Rev. Lett. **63**, 86 (1989); Y. Ajiro *et al.*, *ibid.* **63**, 1424 (1989); M. Date and K. Kindo, *ibid.* **65**, 1659 (1990); M. Hagiwara *et al.*, *ibid.* **65**, 3181 (1990); S.H. Glarum *et al.*, *ibid.* **67**, 1614 (1991); H. Mutka *et al.*, *ibid.* **67**, 497 (1991).

[5]S. Ma, C. Broholm, D. H. Reich, B. J. Sternlieb, and R. W. Erwin, Phys. Rev. Lett. **69**, 3571 (1992).

[6]S. M. Hayden, G. Aeppli, R. Osborn, A. D. Taylor, T. G. Perring, S-W. Cheong, and Z. Fisk, Phys. Rev. Lett. **67**, 3622 (1991).

[7]R. R. P. Singh, P. A. Fleury, K. B. Lyons, and P. E. Sulewski, Phys. Rev. Lett. **62**, 2736 (1989).

[8]R. Saez-Puche, J. M. Coronado, C. L. Otero-Diaz, and J. M. M. Llorente, J. Solid State Chem. **93**, 461 (1991).

[9]S-W. Cheong, A. S. Cooper, L. W. Rupp, Jr., and B. Batlogg, Bull. Am. Phys. Soc. **37**, 116 (1992); J. Darriet and L. P. Regnault, Solid State Commun. **86**, 409 (1993).

[10]P. E. Sulewski and S-W. Cheong, Phys. Rev. B **50**, 551 (1994).

[11]W. P. Lehmann, W. Breitling, and R. Weber, J. Phys. C **14**, 4655 (1981).

[12] H. Shiba, Prog. Theor. Phys. **64**, 466 (1980).

[13]S. Jandl, M. Banville, Q. F. Xu, and A. Ait-Ouali, Phys. Rev. B **46**, 11 585 (1992).

[14]A. Salinas-Sanches, R. Saez-Puche, F. Fernandez, A. de Andres, A. E. Lavat, and E. J. Baran, J. Solid State Chem. **99**, 63 (1992).

[15]A. de Andres, J. L. Martinez, R. Saez-Puche, and A. Salinas-Sanchez, Solid State Commun. **82**, 931 (1992); A. de Andres, S. Taboada, J. L. Martinez, A. Salinas, J. Hernandez, and R. Saez-Puche, Phys. Rev. B **47**, 14 898 (1993).

[16]P. A. Fleury and R. Loudon, Phys. Rev. **166**, 514 (1968).

[17]B. S. Shastry and B. I. Shraiman, Phys. Rev. Lett. **65**, 1068 (1990); Int. J. Mod. Phys. B **5**, 365 (1991).

[18]S. R. White and D. A. Huse, Phys. Rev. B **48**, 3844 (1993).

[19]B. I. Halperin, J. Magn. Magn. Mater. **104-107**, 761 (1992).

[20]R. J. Elliott and M. F. Thorpe, J. Phys. C **2**, 1630 (1969); J. B. Parkinson, *ibid.* **2**, 2012 (1969).

[21]D. P. Arovas and A. Auerbach, Phys. Rev. B **38**, 316 (1988).

[22]T. K. Ng, Phys. Rev. B **45**, 8181 (1992).

[23]I. Affleck and R. A. Weston, Phys. Rev. B **45**, 4667 (1992).

[24]E. S. Sorensen and I. Affleck, Phys. Rev. B **49**, 13 235 (1994); **49**, 15 771 (1994).

[25]S. He (unpublished).

[26]P. Mitra (private communication).

[27]B. Jankó (unpublished).

[28]M. J. Massey, R. Merlin, and S. M. Girvin, Phys. Rev. Lett. **69**, 2299 (1992).

[29]S. L. Cooper and M. V. Klein, Commun. Condens. Matter Phys. **15**, 99 (1990).

[30] A. Zawadowski and B. Jankó (unpublished).

[31]W. Hayes and R. Loudon, *Scattering of Light by Crystals* (Wiley, New York, 1978), p. 272.

[32]P. A. Fleury, Phys. Rev. Lett. **21**, 151 (1968).

[33]S. R. Chinn, H. J. Zeiger, and J. R. O'Connor, Phys. Rev. B **3**, 1709 (1971).

[34]P. A. Fleury and H. J. Guggenheim, Phys. Rev. Lett. **24**, 1346 (1970).

[35]L. J. de Jongh and R. Block, Physica B **79**, 568 (1975).

[36]P. E. Sulewski, P. A. Fleury, K. B. Lyons, S-W. Cheong, and Z. Fisk, Phys. Rev. B **41**, 225 (1990); S. L. Cooper, G. A. Thomas, A. J. Millis, P. E. Sulewski, J. Orenstein, D. H. Rapkine, S-W. Cheong, and P. L. Trevor, *ibid.* **42**, 10 785 (1990).